

of He*. The percentage of Ne* in the neon beam was 43%.

As suggested by the two-state potential curve model⁴ and discussed in more detail previously,^{1(b)} Reaction (3) is associated with transitions from the He*–Ne* potential curve to the He*–Ne curve. Its cross section is designated as $Q_{PI}^{He^*}$. Reaction (2) is associated with transitions between the He*–Ne* and He–Ne* curves with a cross section $Q_{PI}^{Ne^*}$. The total PI cross section is $Q_{PI} = Q_{PI}^{Ne^*} + Q_{PI}^{He^*}$. A total ionization cross section Q_T for the He*–Ne* system is defined as $Q_T \equiv Q_{AI} + Q_{PI}$, where Q_{AI} is the cross section for Reaction (1). The branching ratio is defined as $R \equiv Q_{AI}/Q_T$.

Lab-energy distributions of He* from Reaction (3) were measured and are similar to those previously shown for Ne* from Reaction (2). Information on the reaction kinetics that is derived from these distributions is also similar and includes the following: (a) Reaction (3) is directed with most of the He* scattered in the c.m. system approximately in the direction of the incident He; and (b) $W' > W$ for most of the scattered He*, where W' is the relative KE of the heavy products. This latter fact indicates that the He*–Ne* system is attractive in accord with our previous conclusions.^{1(b)}

A well depth ϵ^* of the He*–Ne* system was previously calculated as $(0.5 \pm 20\%)$ eV using our most accurate method and the distributions of Ne* from Reaction (2).⁵ This method is labeled the min E technique and was applied to the calculation of ϵ^* using the lab-energy distributions of He* from Reaction (3). The result is the same as above.

Relative $Q_{PI}^{He^*}$ are given in Fig. 1. Also included are Q_{AI} , $Q_{PI}^{Ne^*}$, and Q_T . To relate the magnitudes of $Q_{PI}^{He^*}$ and the previously measured Q_{AI} , the ratio $r' = Q_{AI}/Q_{PI}^{He^*}$ was measured at $W = 0.1$ and is designated $r'(0.1)$. The

value of $r'(0.1)$ was determined to be $0.019 \pm 15\%$. It is noted from Fig. 1 that $Q_{PI}^{Ne^*} \gg Q_{PI}^{He^*}$, indicating that the He*–Ne* and He–Ne* systems are more closely coupled than the He*–Ne* and He*–Ne systems.

Absolute cross sections can be obtained from Fig. 1 and the previously measured $Q_{PI}^{Ne^*}(0.1) = 8 \times 10^{-15} \text{ cm}^2$.^{1(a)} For example, $Q_T(0.033) = 142 \times 10^{-16} \text{ cm}^2$ with an estimated error of +53% and –45%. It is also noted that $Q_T \propto W^{-0.40}$.

A curve of R is given in Fig. 2. The $R < 0.5\%$ for all W . The large Q_T , small R , and W dependence of Q_T are characteristic of other attractive systems of two metastables that we have investigated and discussed previously. These systems include He*–He*,^{6(a)} Ar*–Kr*,^{6(b)} and Ne*–Ar*.^{6(c)}

^{a)}Research sponsored by the Air Force Office of Scientific Research (AFSC), U.S. Air Force under Contract F49620-78-C-0015, and by the Office of Naval Research.

¹(a) R. H. Neynaber and G. D. Magnuson, *Phys. Rev. A* **12**, 891 (1975); (b) R. H. Neynaber and S. Y. Tang, *J. Chem. Phys.* **67**, 5619 (1977).

²This percentage of He* is a lower bound as indicated in Table I of R. H. Neynaber, "Merging-Beams Experiments with Excited Atoms," *Electronic and Atomic Collisions*, Invited Papers and Progress Reports XI ICPEAC, edited by N. Oda and K. Takayanagi (North-Holland, Amsterdam, 1980), pp. 287–300.

³C. Reynaud, J. Pommier, Vu Ngoc Tuan, and M. Barat, *Phys. Rev. Lett.* **43**, 579 (1979).

⁴For example, see H. Hotop and A. Niehaus, *Z. Phys.* **238**, 452 (1970) and H. Hotop, *Radiat. Res.* **59**, 379 (1974).

⁵R. H. Neynaber and S. Y. Tang, *J. Chem. Phys.* **69**, 4851 (1978).

⁶(a) R. H. Neynaber, G. D. Magnuson, and S. Y. Tang, *J. Chem. Phys.* **68**, 5112 (1978); (b) R. H. Neynaber and S. Y. Tang, *ibid.* **71**, 3608 (1979); (c) R. H. Neynaber and S. Y. Tang, *J. Chem. Phys.* (to be published).

On the optimum trajectory in semiclassical calculations of inelastic collisions

Robert J. Gordon

Department of Chemistry, University of Illinois at Chicago, Chicago, Illinois 60680
(Received 23 August 1979; accepted 20 December 1979)

A prescription used in many semiclassical formulations of molecular scattering theory is to calculate the translational motion classically while treating the internal coordinates quantum mechanically. A classical trajectory is used to determine the time dependence of the intermolecular potential, which is then inserted into the quantal equations for the internal degrees of freedom. The question then arises as to which trajectory to use. In order to guarantee microscopic reversibility, a common procedure is to choose some average initial trans-

lational energy, such that the trajectories connecting the initial and final quantal states are the same in both directions. Three frequent choices are the arithmetic mean of the velocities associated with the initial and final states (v_a),^{1–8} the arithmetic mean of the initial and final translational energies (E_a),^{9–13} and the geometric mean of the velocities (v_g).^{14–18} Giese and Gentry⁴ and Billing⁵ showed that the v_a approximation is much more accurate than v_g in collinear collisions at low energies. Here we present a simple argument justifying the use of

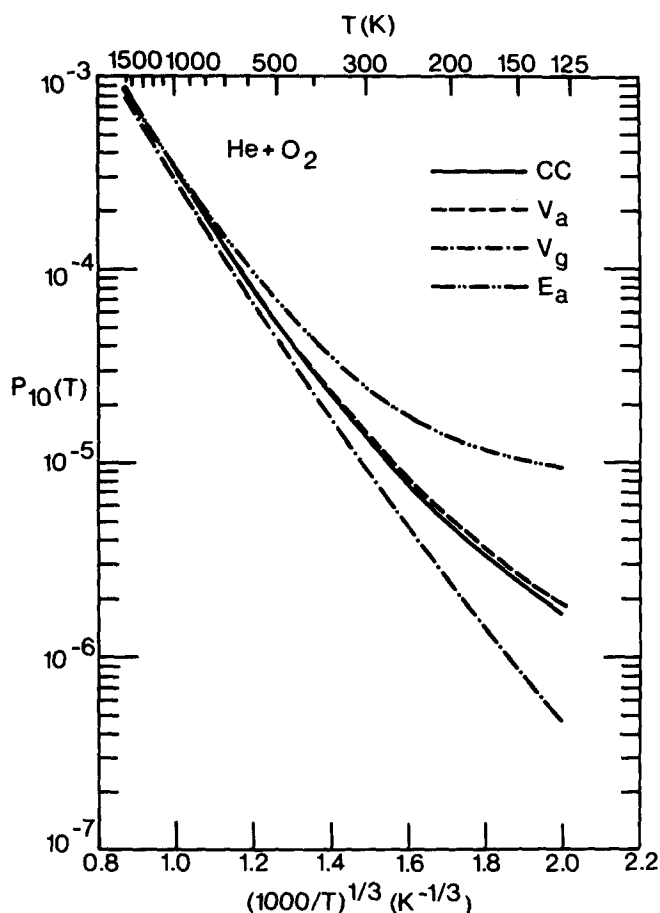


FIG. 1. Comparison of the semiclassical approximations, using the arithmetic mean of the velocities (v_a), geometric mean of the velocities (v_g), and the arithmetic mean of the energies (E_a), with exact quantal calculations (CC) for the system He + O₂ ($v = 1$). The forced oscillator model was used with an isotropic Lennard-Jones intermolecular potential.

the v_a approximation.

Consider a transition from state m to state n . Using radial JWKB wave functions to simplify the close coupled equations,^{15,16} one obtains the classical path equations, which can be written in the form

$$i\hbar dc_n/dR = \sum_j \{V_{j,n}(R)/(v_j(R)v_n(R))^{1/2}\} \exp(i(S_j - S_n)/\hbar). \quad (1)$$

In Eq. (1) c_n is the amplitude of state n ; $V_{j,n}(R)$ is the matrix element of the intermolecular potential averaged over the internal coordinates of states j and n at radial distance R ; $v_j(R)$ is the velocity and $S_j(R)$ the action integral associated with the JWKB wave function for state j at distance R . In numerical work uniform JWKB wave functions must be used to treat the turning point properly.¹⁵ The ordinary JWKB function is used here to emphasize the oscillatory behavior of Eq. (1). These equations can be uncoupled to first order, giving

$$i\hbar c_n = \int_{-\infty}^{\infty} [V_{mn}(x)/v_g(x)] \exp\left\{i\omega_{mn} \int_0^x v_a(x')^{-1} dx'\right\} dx. \quad (2)$$

In Eq. (2) x is the distance from the classical turning point for either state; $v_g(x)$ and $v_a(x)$ are, respectively,

the geometric and arithmetic means of velocities $v_m(x)$ and $v_n(x)$; and $\hbar\omega_{mn}$ is the difference between the initial and final internal energies.² We now transform the independent variable from distance to time by choosing a classical path. Let this path be denoted by $x(t)$, with $x(0) = 0$ and $v(t) = dx/dt$. Eq. (2) then becomes

$$i\hbar c_n = \int_{-\infty}^{\infty} V_{mn}(x(t)) [v(t)/v_g(x(t))] \times \exp\left\{i\omega_{mn} \int_0^t [v(t')/v_a(x'(t'))] dt'\right\} dt. \quad (3)$$

We observe that Eq. (3) resembles the result of ordinary time dependent perturbation theory.^{2,14-16} The correspondence is improved if the classical trajectory is chosen such that either $v(t) \approx v_a(x(t))$ or $v(t) \approx v_g(x(t))$. In particular, Lawley and Ross¹⁴ recommended the geometric approximation. It should be noted, however, that the pre-exponential factor in the outer integral is strongly peaked at $x = 0$ and is insensitive to the choice of trajectory. On the other hand, the exponential function oscillates rapidly and will have the proper frequency only for $v(t) \approx v_a(x(t))$. For isotropic potentials this condition can be fulfilled by using the arithmetic mean of the initial and final velocities. For highly anisotropic potentials it may be difficult to satisfy either condition. There does not appear to be any justification for the E_a approximation other than its convenience for thermal averaging.

A second point we wish to make is that use of either the v_g or the E_a approximation can lead to significant errors in the interpretation of experimental rate constants. We illustrate this point with a model calculation of the vibrational relaxation of O₂($v = 1$) by He. A harmonic oscillator with an isotropic Lennard-Jones potential was assumed, with parameters²⁰ $\sigma = 5.962 \text{ \AA}$ and $\epsilon = 25.17 \text{ cm}^{-1}$. Cross sections for vibrational relaxation were calculated with the forced oscillator (INDECENT) semiclassical model⁴ and also by integrating the exact close coupled (CC) quantal equations.²¹ The thermally averaged transition probabilities, $P_{10}(T)$, resulting from the v_a , v_g , and E_a approximations are compared with the CC results in Fig. 1. Excellent agreement between the v_a and CC calculations is obtained over a wide range of temperatures. Below room temperature the v_g approximation significantly underestimates P_{10} , while the E_a approximation overestimates it. Moreover the E_a approximation exaggerates the departure from $T^{-1/3}$ behavior at low temperatures. Qualitatively similar results were obtained for He + Co($v = 1$) using the Landau-Teller semiclassical model.²⁰ This system was the subject of a recent pair of Comments.^{7,11(b)} Our calculations show that most of the curvature in Ref. 11(b) is due to the use of the E_a approximation.²²

Support by the National Science Foundation and by the Computer Center of the University of Illinois at Chicago are gratefully acknowledged. We wish to thank Dr. A. F. Wagner for use of his CC computer program. We have enjoyed a useful discussion with Prof. E. A. Gislason.

- ¹T. L. Cottrell and J. C. McCoubrey, *Molecular Energy Transfer in Gases* (Butterworths, London, 1961).
²D. Rapp, *J. Chem. Phys.* **40**, 2813 (1964).
³R. D. Levine and B. R. Johnson, *Chem. Phys. Lett.* **8**, 501 (1971).
⁴W. R. Gentry and C. F. Giese, *J. Chem. Phys.* **63**, 3144 (1975).
⁵G. D. Billing, *J. Chem. Phys.* **64**, 908 (1976).
⁶G. D. Billing, *Chem. Phys. Lett.* **50**, 320 (1977).
⁷T. J. Price and C. J. S. M. Simpson, *J. Chem. Phys.* **66**, 1385 (1977).
⁸D. A. Copeland, *J. Chem. Phys.* **69**, 3005 (1978).
⁹B. Stevens, *Collisional Activation in Gases* (Pergamon, Oxford, 1967).
¹⁰H. K. Shin, *J. Phys. Chem.* **75**, 1079 (1971).
¹¹(a) W. A. Wassam, Jr. and R. D. Levine, *J. Chem. Phys.* **64**, 3118 (1976); (b) **66**, 1387 (1977).
¹²G. D. Billing, *Chem. Phys.* **30**, 387 (1978).
¹³R. L. McKenzie, *J. Chem. Phys.* **63**, 1655 (1975).
¹⁴K. P. Lawley and J. Ross, *J. Chem. Phys.* **43**, 2930 (1965).
¹⁵R. J. Cross, Jr., *J. Chem. Phys.* **51**, 5163 (1969).
¹⁶J. B. Delos, W. R. Thorson, and S. K. Knudson, *Phys. Rev. A* **6**, 720 (1972); J. B. Delos and W. R. Thorson, *Phys. Rev. A* **6**, 720 (1972).
¹⁷G. D. Billing, *Chem. Phys. Lett.* **30**, 391 (1975).
¹⁸S. L. Davis and J. E. Boggs, *J. Chem. Phys.* **69**, 2355 (1978).
¹⁹G. Breit and P. B. Daitch, *Proc. Natl. Acad. Sci.* **41**, 653 (1955).
²⁰R. J. Gordon, *J. Chem. Phys.* **65**, 4945 (1976).
²¹A. F. Wagner and V. McKoy, *J. Chem. Phys.* **57**, 2998 (1972).
²²D. C. Allen, T. J. Price, and C. J. S. M. Simpson, *Chem. Phys.* **41**, 449 (1979).

Analytic formula for chemically induced magnetic polarization by $S-T_{\pm 1}$ mixing in a strong magnetic field^{a)}

F. J. Adrian and L. Monchick

Milton S. Eisenhower Research Center, Applied Physics Laboratory, The Johns Hopkins University, Laurel, Maryland 20810

(Received 17 December 1979; accepted 5 February 1980)

Recently we reported a theory of chemically induced magnetic polarization due to mixing of the singlet (S) and $M_S = \pm 1$ triplet sublevels ($T_{\pm 1}$) of a diffusing radical pair in a strong magnetic field,¹ which paper is henceforth referred to as AM. The polarization, due almost completely to $S-T_{-1}$ mixing in the level crossing region, was expressed as a complicated series which had to be evaluated numerically. Here, we derive an analytic formula for this polarization, whose very strong field limit corresponds to Alexandrov's result for nonadiabatic transitions between two linearly intersecting energy levels.²

By Eq. (35) of AM, the $t \rightarrow \infty$ limit of the polarization produced by $S-T_{-1}$ mixing is

$$\mathcal{P}_{\infty}(S-T_{-1}) = \frac{a^2}{2H^2} - \frac{a^2}{4} \int_{r_0=1}^{\infty} dp \int_{q=1}^{\infty} dq \times [G_{+,t}(p, q) + G_{*,t}(p, q)], \quad (1)$$

where a and H are, respectively, related to the hyperfine interaction, which mixes the S and T_{-1} states, and the magnetic field [cf. Eq. (6) of AM], and $G_{*,t}$ is a Green function. The $S-T_{-1}$ polarization is obtained by changing the sign of the rhs of Eq. (1) and also the sign of H , where the dependence of $G_{*,t}$ on H will be given momentarily.

We now replace the truncated Green function $G_{*,t}$ in Eq. (1) by the complete function G_* , and drop the $a^2/2H^2$ term, which is included in G_* but had to be treated separately in AM because of integral convergence problems. Usually, the exponentially decaying exchange interac-

tion, which splits the S and T states, will be very large at the minimum interradical separation [i.e., $(J_0 e^{-\lambda r})_{r=1} \rightarrow \infty$], in which case Eq. (23) of AM shows that

$$G_*(p, q) = -\frac{2}{\lambda} \int_0^{\infty} \frac{x \mathcal{J}_{\nu}(x | \omega | e^{-\lambda p/2}) \mathcal{J}_{\nu}(x | \omega | e^{-\lambda q/2}) dx}{x^2 + i}, \quad (2)$$

where \mathcal{J}_{ν} is the Bessel function of order ν , and by Eqs. (15) and (18) of AM with $s \rightarrow 0$, which corresponds to the long-time limit,

$$\omega = (4J_0/\lambda^2)^{1/2} e^{-\lambda r/4}; \quad \nu = (4H/\lambda^2)^{1/2} e^{-\lambda r/4}. \quad (3)$$

TABLE I. ($S-T_{\pm 1}$) polarization as a function of H_0 and λ . Other parameters are $D = 2(10)^{-5}$ cm/sec, $\sigma = 2(10)^{-8}$ cm, $\tilde{r}_c = \sigma r_c$, $\tilde{\lambda} = \lambda/\sigma$, and $2\tilde{J}_0 e^{-\tilde{\lambda} \sigma} = 4(10)^{13}$ rad/sec.

| H_0 G | λ | r_c | $\nu/e^{-\lambda r/4}$ | $\Delta \mathcal{P}_{\infty}(S-T_{\pm 1})/a^2$ | |
|---------|-----------|-------|------------------------|--|---------------------|
| | | | | Eq. (6) $ \nu \rightarrow \infty$ | Eq. (6) \equiv AM |
| 850 | 2 | 4.944 | 0.547 | 12.98 | 13.59 |
| 3400 | 2 | 4.251 | 1.094 | 2.79 | 2.82 |
| 13600 | 2 | 3.588 | 2.187 | 0.58 | 0.58 |
| 850 | 4 | 2.972 | 0.273 | 3.90 | 4.56 |
| 3400 | 4 | 2.626 | 0.547 | 0.86 | 0.90 |
| 13600 | 4 | 2.279 | 1.094 | 0.19 | 0.19 |
| 850 | 8 | 1.986 | 0.137 | 1.30 | 1.79 |
| 3400 | 8 | 1.813 | 0.273 | 0.30 | 0.34 |
| 13600 | 8 | 1.639 | 0.547 | 0.067 | 0.069 |
| 850 | 16 | 1.493 | 0.068 | 0.49 | 0.80 |
| 3400 | 16 | 1.406 | 0.136 | 0.12 | 0.15 |
| 13600 | 16 | 1.320 | 0.273 | 0.027 | 0.030 |